

Turbulent, Concurrent, Ceiling Flame Spread: The Effect of Buoyancy

L. ZHOU and A. C. FERNANDEZ-PELLO*

Department of Mechanical Engineering, University of California, Berkeley, CA 94720

Experiments have been conducted to study the effects of forced air flow velocity and grid-generated turbulence on the flow-assisted flame spread over a flat solid combustible surface in a ceiling configuration. The tests are conducted with thick PMMA sheets as fuel, and air as oxidizer. Flame spread rate, flame length, surface heat flux, and products composition are obtained for air flow velocities ranging from 0.25 to 4.5 m/s and turbulence intensities the 1% to 15%. It is found that for all turbulence intensities the ceiling flame spread rate increases with the flow velocity, and that the flow turbulence retards the flame spread for flow velocities larger than 1 m/s and enhances it at lower velocities. The flame length and the surface heat flux exhibit power law correlations with the fuel pyrolysis length, and the flame spread rate data can be correlated with an expression deduced from a simplified heat transfer analysis of the process. In order to determine the effect of buoyancy on the flame spread processes, data from the ceiling configuration experiments are compared with data from floor tests conducted previously. The experimental results indicate that in ceiling spread, buoyancy has two main competing effects. One is an enhancement of the heat transfer from the flame to the solid surface because the flame stands closer to the surface, the other is an incomplete combustion caused by larger heat losses to the wall and boundary layer stratification. For large flow velocities (larger than 1 m/s), the enhanced heat transfer is found to be dominant and results in a faster flame spread in the ceiling than in the floor. For small flow velocities, the incomplete combustion becomes more important and the opposite result is observed. The species concentration data show that in general the combustion reaction is less complete in ceiling spread than in floor spread, and that significant amounts of CO and unburned hydrocarbons are produced in ceiling flame spread.

INTRODUCTION

The study of the spread of flames over solid combustible surfaces has attracted much attention over the past few years. One of the main motivations to conduct such a study comes from its direct applications in fire safety research. Solid combustible materials are widely used in various buildings, especially as interior surfaces which provide the routes for flames to propagate through the building in accidental fires. Although the controlling mechanisms of flame spread are similar for the different surface orientations (floor, wall, and ceiling), significant differences do arise. Buoyant flows generated by flames often contribute to these differences. For example, in the case of a diffusion flame spreading over a horizontal surface in a forced flow, buoyancy drives the flame

upward, raising the flame from the surface if it is spreading over a floor or pushing it closer to the fuel surface if spreading over a ceiling. The change in the flame standoff distance alters the magnitude of heat transfer from the flame to the solid, and possibly affects the gas-phase combustion reaction thorough cold wall effects, which in turn influences the rate of flame spread. In a forced oxidizing flow, the extent of the buoyancy effect depends on the relative magnitudes of natural and forced convection. Normally the buoyancy effects are more significant when the forced flow velocity is small, or the length scale is large.

Flame spread is often characterized as opposed or concurrent (or flow-assisted) according to whether the oxidizing flow moves in the opposite or the same direction of flame propagation. The concurrent or flow-assisted flame spread has been studied intensively because its rapid and hazardous propagation speed. Some excellent reviews on this subject are available

*Corresponding author

[1–4]. The accompanying oxidizer flow can be induced naturally by buoyancy, or by pressure gradients that are externally generated by air currents or ventilation in buildings, or by both effects, as in most real fires. In most studies of concurrent flame spread, the solid combustible is placed in a vertical (wall) or horizontal face-up (floor) position. The vertical wall geometry is frequently studied because of its close connection with fire development. The buoyancy-driven oxidizer flow in this mode of flame spread can be either laminar [5] or turbulent [6], depending on the wall height [7]. The horizontal face-up (floor) configuration is utilized mostly for forced-flow flame spread studies [8, 9]. The parameters frequently investigated in concurrent flame spread studies are the flame spread rate, surface heat flux, and flame length, the latter two because of their influence in determining the rate of spread. Studies have been conducted for their dependence on external conditions such as the forced flow velocity, turbulence intensity, oxygen concentration, and external radiation. It is found that concurrent flame spread is controlled chiefly by the heat transfer from the diffusion flame to the solid fuel surface. The gas-phase chemistry affects the spread rate through the flame temperature, or rate of heat release, which in turn affect the heat transferred to the fuel surface.

In contrast to the abundance of the research performed on floor and vertical wall flame spread, only a few fundamental flame spread studies have been conducted with a ceiling configuration [10, 11], to the best knowledge of the authors. Mao and Fernandez-Pello [10] studied the spread of flames in a vertical wall ceiling corner, and observed the effect of the vertical wall height and ceiling length on the flame spread rate over the wall and ceiling. Recently, Mekki et al. [11] conducted experiments of the laminar, forced-flow flame spread over charring wood and noncharring PMMA surface in the ceiling configuration. They found that the flame spread rates for both materials varied nearly linearly with the free stream velocity as predicted by the theoretical models. The ASTM E84 tunnel test [12] also employs a low velocity ceiling configuration for material fire environment evaluation.

The scarce information currently available

on the controlling mechanisms of ceiling flame spread and the potential significance of such knowledge in fire prevention and protection have provided the main incentives for conducting the present study. The objective here is to carry out systematic experiments to investigate the effect of the flow velocity and turbulence intensity on the ceiling flame spread process, and to determine the buoyancy effect on the horizontal flame spread by comparing the experimental results from ceiling and floor configurations. Previous floor experimental data [13] together with additional new floor flame spread tests performed in low-velocity flows are utilized in the study.

EXPERIMENT

A schematic of the experimental apparatus is shown in Fig. 1. It consists of a laboratory-scale wind tunnel designed for condensed fuel flame propagation experiments under various flow conditions, and the supporting diagnostic instrumentation. The wind tunnel consists of three main sections: the settling chamber with converging nozzle, the test section and the exhaust section. The settling chamber, 0.89 m long, supplies oxidizer flow to the test section through a converging nozzle with an area reduction ratio of 5.6 to 1. The test section is 0.61 m long and has a rectangular cross section that is 127 mm wide and 76.2 mm high. The side walls of the test section are made of 6.3-mm-thick Pyrex glass for visual observation and optical diagnostic access. The floor and ceiling of the test section are made of 55-mm-thick Marinite slabs, and are designed to mount in them the fuel specimen. The test section is followed by the exhaust section, 1.22 m long and with a cross-sectional area the same as the test section. Inside this section are four mixing plates of different geometric shapes placed perpendicular to the flow direction to mix the exhaust gases and produce a uniform concentration distribution. Exhaust gas samples are taken from the exit of the exhaust section for species concentration measurements. The wind tunnel, the test section and the exhaust section are mounted horizontally on a three-axis positioning table, while the optical instrumentation is kept stationary.

The air flow in the test section is supplied from a centralized air compressor and the flow rate controlled with precision valves. Turbulence is introduced to the flow by means of perforated plates that are placed perpendicular to the flow direction at the exit of the tunnel converging nozzle. A prescribed turbulence intensity is obtained through a combination of flow velocity and plate blockage ratio. The flow velocity and turbulence intensity distributions are measured with a one-component laser doppler velocimeter operating in dual-beam, forward scattering mode. A detailed description of the velocity and turbulence intensity profiles through the test section can be found from previous work [14]. The diagnostic installation also includes a schlieren system with a 0.45-m-diameter collimated light beam and an array of eight k-type thermocouples placed evenly on the fuel surface along the centerline. The thermocouples are used to measure and monitor the solid combustible surface temperatures. Gas analyzers are used to measure the concentrations of major species O_2 , CO , CO_2 , NO (Horiba, Infrared) and unburned hydrocarbons (Horiba-flame ionization) in the exhaust gas flow.

The fuel specimens used in this work are

made from 12.7-mm-thick PMMA (Polymethylmethacrylate) sheets manufactured by Roam and Haas (Plexiglas G), 0.306 m long and 60 mm wide. PMMA is chosen for the study because of its well-known and uniform properties and noncharring burning. The PMMA sheets are mounted flush in the Marinite ceiling or floor of the tunnel test section. The specimen is ignited at its upstream edge with an electrically heated Nichrome wire that initiates the flame spread uniformly over the whole width of the PMMA sheet. The flame spread rate along the PMMA sheet is calculated from the time interval needed for the pyrolysis front to travel the fixed distance between two consecutive thermocouples. Thus, seven values of the flame spread rate are obtained from the eight surface thermocouples outputs. These spread rates are then compared to determine if the flame front accelerates or decelerates as it progresses along the sample surface.

RESULTS AND DISCUSSION

Flow velocity and turbulence

Measured ceiling flame spread rates over the PMMA surface are plotted in Fig. 2 versus the

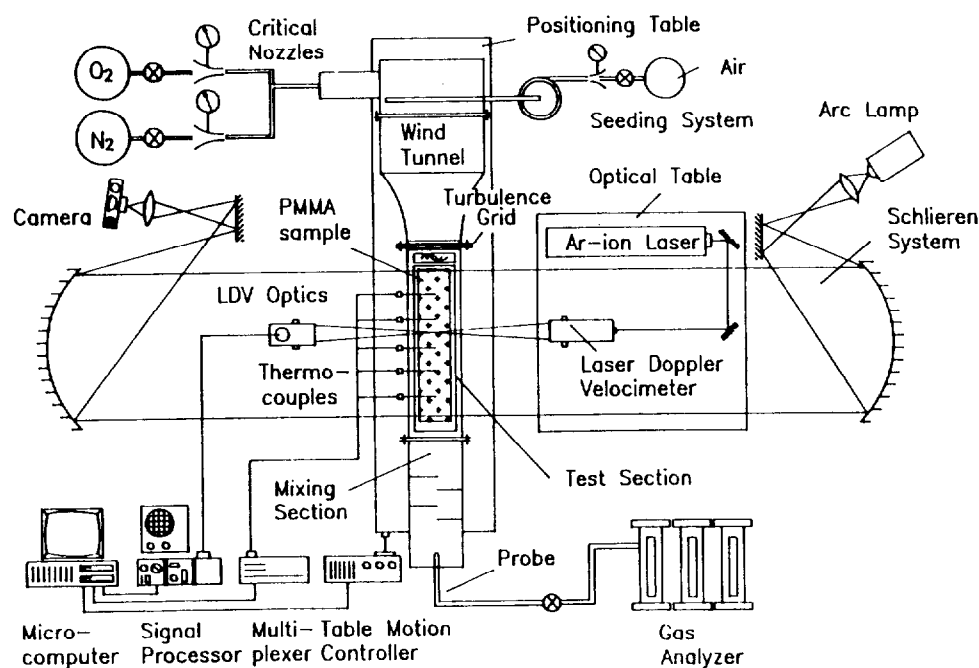


Fig. 1. Schematic of the experimental facility.

external flow velocity for several turbulence intensities. The spread rate reported is an average of the values calculated from consecutive thermocouples throughout the specimen length and from three different tests. The standard deviation is, in most cases, of the order of 7%. No increasing or decreasing trend could be inferred from the flame spread rate measurements along of the sample and, consequently, the spread rate was considered as constant throughout the sample. The flow velocity in the experiments ranges from 0.25 to 4.5 m/s and the turbulence intensity from 1% to 15%. At velocities larger than 4.5 m/s, it was very difficult to ignite the PMMA and signs of extinction were observed at the upstream flame leading edge. It is seen from Fig. 2 that the flame spread rate increases with the flow velocity for all turbulence conditions tested. Similar dependence of the spread rate on the flow velocity was observed in the floor configuration experiments conducted previously [13]. The monotonic increase of the flame spread rate

with the flow velocity is also in qualitative agreement with the predictions by most theoretical models of concurrent flame spread [3]. As the flow velocity is increased, the thermal boundary layer becomes thinner and the diffusion flame is pushed closer to the fuel surface. This enhances the heat transfer from the flame to the solid combustible, and, as a result, the flame spread rate.

The dependence of the ceiling flame spread rate on the flow turbulence is shown in Fig. 3. The turbulence effect can be divided into two regions based on the flow velocity. For flow velocities larger than 1 m/s, the flame spread rate decreases with increased flow turbulence; this is consistent with the previous experimental results for floor flame spread. The decrease of the flame spread rate is mainly caused by a shortened flame length at higher flow turbulence levels. The exhaust gas analysis indicates that the flame shortening is the result of the enhanced combustion in high-turbulence intensity flows, which is discussed further in the

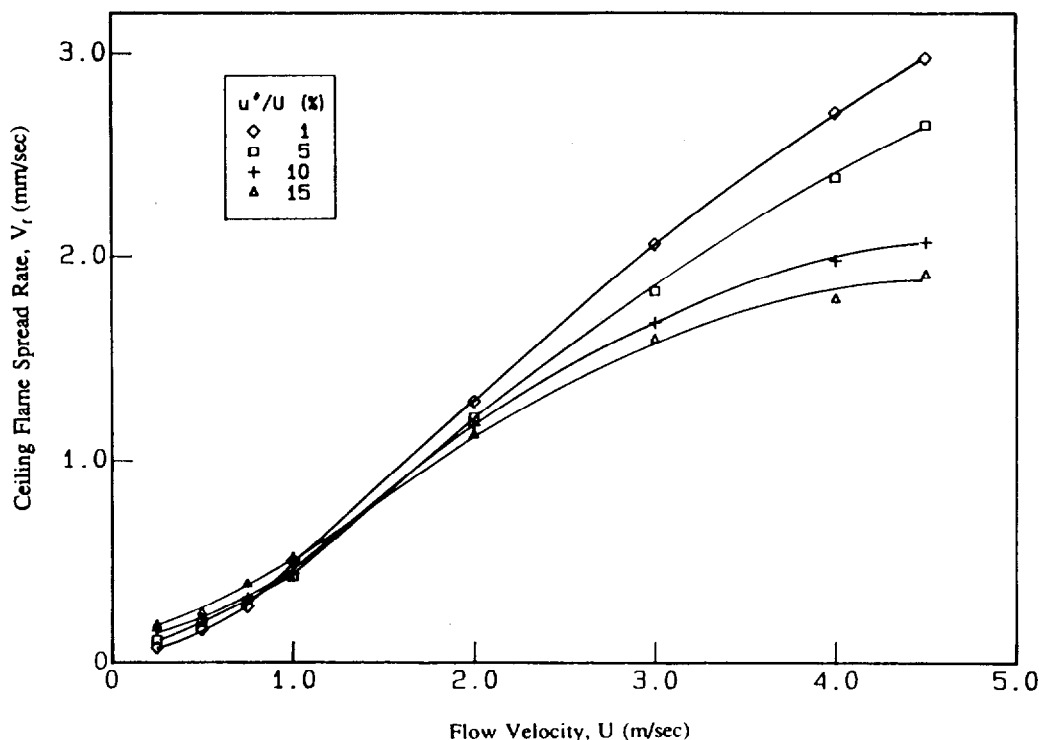


Fig. 2. Dependence of the PMMA ceiling flame spread rate on the free stream flow velocity for several values of the turbulence intensity.

next section with the exhaust gas concentration measurements (Fig. 9–12). At low flow velocities, however, the enhancing effect of turbulence on the flame spread rate becomes less pronounced, as seen in Fig. 3. For flows with velocities less than 0.75 m/s, the flame spread rate increases slightly with the flow turbulence intensity, which was not observed in the floor configuration tests. This transition seems to occur around flow velocities of the order of 1 m/s. As will be explained in more detail later, a possible reason for this change in the turbulence effect on the flame spread rate is that for low velocity flows, buoyancy reduces the flame standoff distance to the surface and stratification and quenching effects become important [15,16]. Increasing flow turbulence reduces the flow stratification and enhances the combustion with more vigorous mixing [13]; this increases the flame temperature and the heat transfer to the combustible surface, and as a result, the flame spread rate.

In order to interpret the experimental results, it is convenient to briefly examine the

mechanisms controlling the spread of a flame over a solid combustible. Previous experimental and theoretical work on concurrent flame spread [1–4] has indicated that heat transfer from the flame to the solid fuel is the dominant controlling mechanism. A simple energy analysis applied to a control volume in the unburned solid, downstream from the pyrolysis front, provides an expression for the flame spread rate that seems to describe the spread process well [17]. Assuming that the solid behaves as though it is semiinfinite, that the heat flux from the flame to the solid, q_f , is constant throughout the downstream flame length, l_f , and that the solid pyrolyzes and ignites when its surface temperature reaches the pyrolysis temperature, T_p , the following expression is then obtained for the flame spread rate, V_f [17]:

$$V_f = \frac{4q_f^2 l_f}{\pi k \rho c (T_p - T_i)^2}, \quad (1)$$

where T_i is the initial solid temperature and $k \rho c$ is the thermal inertia of the solid. This

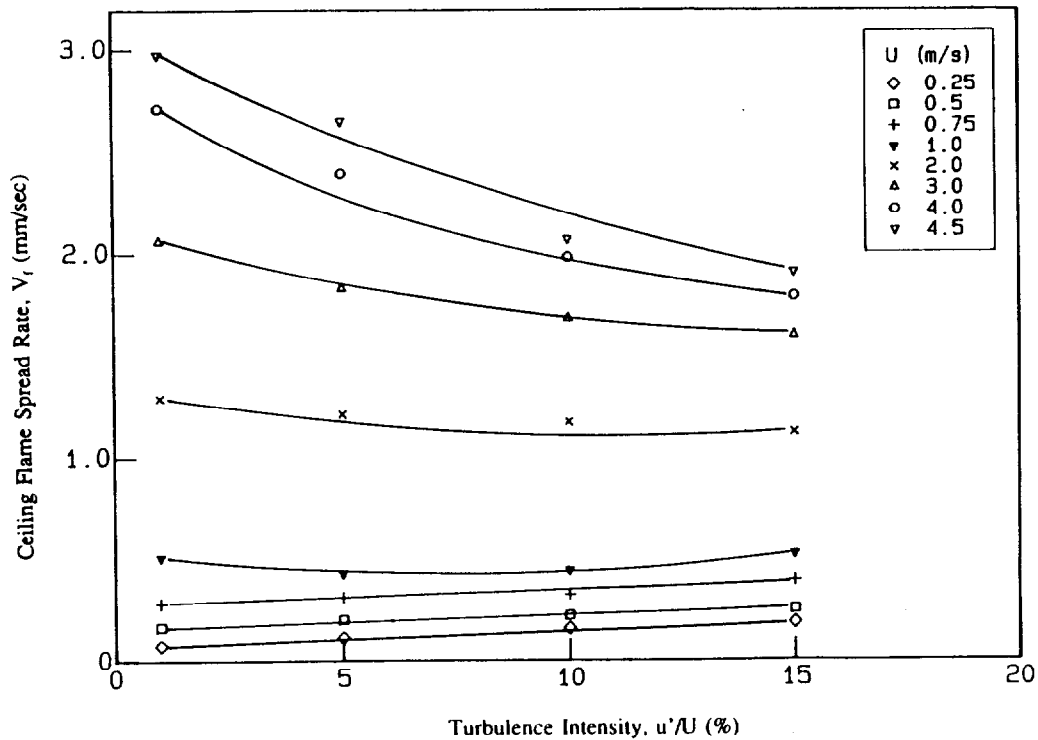


Fig. 3. Variation of the PMMA ceiling flame spread rate with the turbulence intensity for several values of the free stream flow velocity.

equation, which applies to any geometry, shows that the flow velocity and turbulence intensity can affect the flame spread rate primarily through the surface heat flux and the flame length. Other mechanisms related to heat flux variations and transients may have indirect influences on Eq. 1.

In this work, the flame length and surface heat flux have been determined from the solid surface temperature histories. Their relation to the pyrolysis length is an important aspect of the flame spread problem [3]. In the calculation, the pyrolysis length is determined from the location of the thermocouple which has just reached the pyrolysis temperature. The flame length at this moment is obtained by determining the location of the thermocouple whose temperature is starting to rise. It should be noted that the calculated length is not necessarily the actual visible flame length, but the length of the surface downstream of the pyrolysis front with elevated temperatures. For simplicity, this length is called the flame length. The calculated flame length changes not only with the flow velocity and turbulence intensity, but also with the pyrolysis length, l_p . The general trend is that the flame length increases with the pyrolysis length and the flow velocity, and decreases with the flow turbulence.

Following previous studies on the subject [18–20], a power law correlation between the flame length and pyrolysis length is sought here. A typical set of flame length and pyrolysis length data is shown in Fig. 4 for flow velocity ranging from 0.25 to 4 m/s. It can be seen that the flame length increases with the flow velocity, and that there is a power law

correlation between the flame length and the pyrolysis length. The logarithmic fit of the two lengths yields

$$l_f = al_p^b \quad (2)$$

where a and b vary with the flow conditions. Table 1 gives the coefficient a and power b as functions of the flow velocity and turbulence intensity for ceiling flame spread. The values are averaged of those obtained along the length of the PMMA sheet.

The other important parameter, the surface heat flux in the unburned region downstream from the pyrolysis front, can be calculated from the solid surface temperature histories with the assumption that the solid fuel slab behaves as a semiinfinite medium exposed to a constant heat flux. This method is applied to the temperature data provided by eight thermocouples along the longitudinal axis of the solid surface. Typical results are shown in Fig. 5 versus the pyrolysis length for a flow turbulence intensity of 5% and flow velocities from 0.25 to 4 m/s. The correlation between the surface heat flux and the pyrolysis length can also be summarized as a power law:

$$q_f^2 l_p^c = d, \quad (3)$$

where c and d are functions of the flow velocity and turbulence. Table 2 shows the values of the power c and coefficient d for different flow conditions of ceiling flame spread.

Even though both the flame length and surface heat flux are functions of the pyrolysis length (namely, time), the resulting product $q_f^2 l_f$ is, however, approximately constant along the solid fuel surface. From Tables 1 and 2, it

TABLE 1
The Dependence of a and b in Eq. 2, $l_f = al_p^b$, on the Flow Conditions (Ceiling)

Turbulence Intensity		Flow Velocity U (m/s)						
		0.25	0.5	0.75	1.0	2.0	3.0	4.0
1%	a	6.8	7.5	7.0	8.5	9.4	10.0	11.0
	b	0.70	0.70	0.73	0.77	0.78	0.81	0.84
5%	a	5.2	6.5	6.0	6.0	6.5	6.0	6.8
	b	0.74	0.77	0.78	0.81	0.84	0.86	0.88
10%	a	6.0	6.2	6.0	5.2	6.5	5.3	5.4
	b	0.77	0.80	0.80	0.81	0.82	0.85	0.90
15%	a	4.0	4.4	6.0	5.5	5.0	6.0	6.4
	b	0.80	0.80	0.81	0.82	0.84	0.85	0.90

is easy to see that the power exponents b and c are quite close, and that the product, $q_f^2 l_f$ is practically independent of the pyrolysis length, l_p . This result is interesting, and in qualitative agreement with forced flow boundary layer heat transfer predictions when flame radiation is neglected [3]. Since $q_f^2 l_f$ does not change considerably during the entire course of flame spread in these tests, it is possible to use the experimental data to verify the predictive capability of Eq. 1. The measured flame spread rate and the calculated flame length and heat flux data are combined to produce Fig. 6, where the nondimensional flame spread rate deduced from Eq. 1 is plotted versus the flow turbulence intensity for the flow velocity from 0.25 to 4 m/s. The final result is quite good particularly considering the simple assumptions used in deducing the equation and the diversity of the measurements. The deviation of the nondimensional flame spread rate from unity and the scatter on the correlation are attributed mainly to the approximate nature of the

method of determining the flame length and the surface heat flux and the selection of the properties T_p and $k\rho c$ of PMMA (taken as constants here, $T_p = 663$ K, $k = 1.99 \times 10^{-2}$ J/smK, $\rho = 1.19$ kg/m³, $c = 1.46 \times 10^3$ J/kgK).

It should be noted that the present tests were conducted in a small-scale experimental facility and that the flames were relatively thin and not strongly radiative [7]. However, as the scale of the fuel sample is increased, the flames become thick and radiative, and they rise from the floor due to the buoyancy [9]. This occurs because buoyancy is strongly dependent on the flame length size ($Gr \propto l_f^3$). In such cases, radiation becomes the dominant heat transfer mode and the flame spread rate would vary accordingly. In large-scale ceiling flame spread, it is expected that the spreading process would have similar characteristics as the small scale tests, with relatively thin cellular flames in a stable boundary layer [21] and strong quenching effects from the wall. Further discussion on

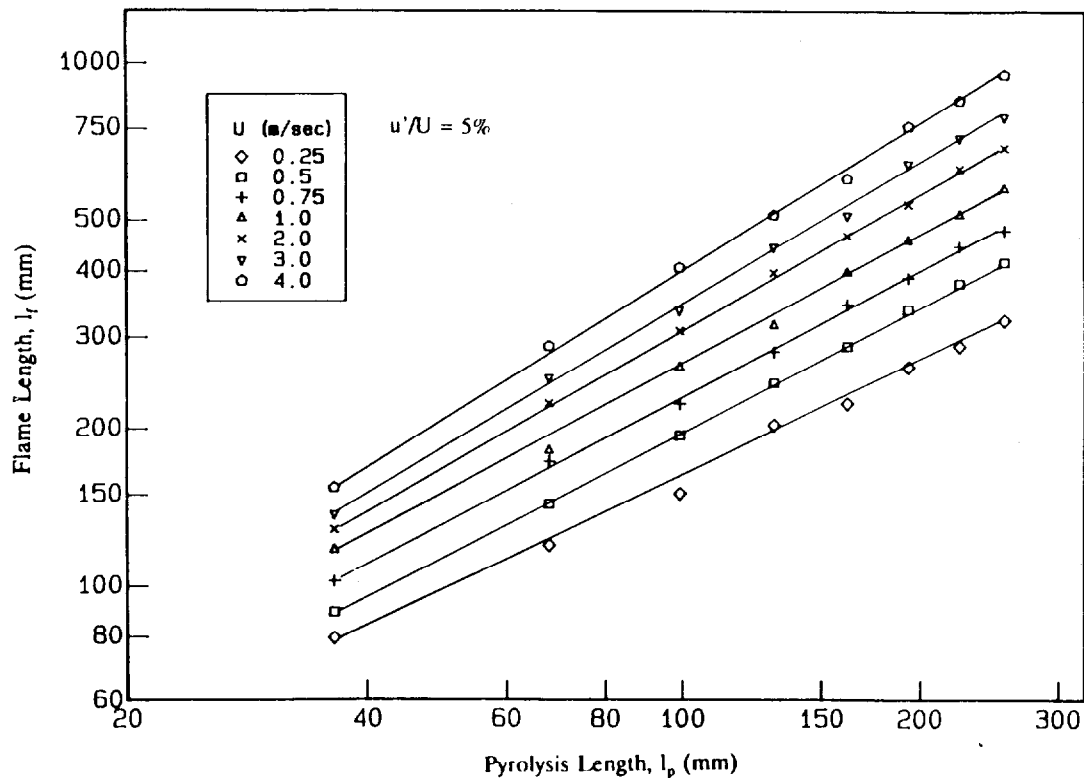


Fig. 4. Dependence of the flame length on the pyrolysis length for several flow velocities and a turbulence intensity of 5% for ceiling flame spread.

the buoyancy effect is conducted in the next section.

Buoyancy effect

Since concurrent flame spread is mainly controlled by heat transfer from the flame to the solid, the buoyancy effect on flame spread can be studied by investigating its influence on the parameters affecting this heat transfer. Buoyancy pushes the flame closer to the fuel surface in ceiling flame spread and lifts the flame away from the fuel surface in floor spread. Therefore, buoyancy can change the magnitude of the heat transfer from the flame to the fuel by altering the distance between the flame and the solid surface, which would result in an increased heat flux in the ceiling configuration, and a decreased heat flux for the floor. Consequently, the flame spread rate should be enhanced in the former case and hindered in the latter. However, in the ceiling case the thermal stratification and quenching effects on the

combustion reaction can inhibit the flame spread process [15]. The stable characteristics of the thermal layer in the ceiling configuration, versus the unstable thermal layer in the floor case, can affect the turbulent mixing of the fuel vapor and oxidizer at the reaction zone. Whether buoyancy will enhance or deter flame spread depends on which effect is dominant in a particular test condition [15]. Examples of the ceiling floor boundary layer characteristics are shown in the schlieren images of Fig. 7, taken under the flow condition of $U = 2$ m/s and $u'/U = 1\%$. These schlieren images show that the thermal boundary layer is thinner in the ceiling than in the floor. Video recordings of these images also show that the flame is more stable in the ceiling.

To show the buoyancy effect on the horizontal flame spread rate, ceiling and floor flame spread rate data are compared in Fig. 8. Two turbulence conditions of 1% and 15% are used to represent low- and high-turbulence cases, respectively. It is seen that for flows with a

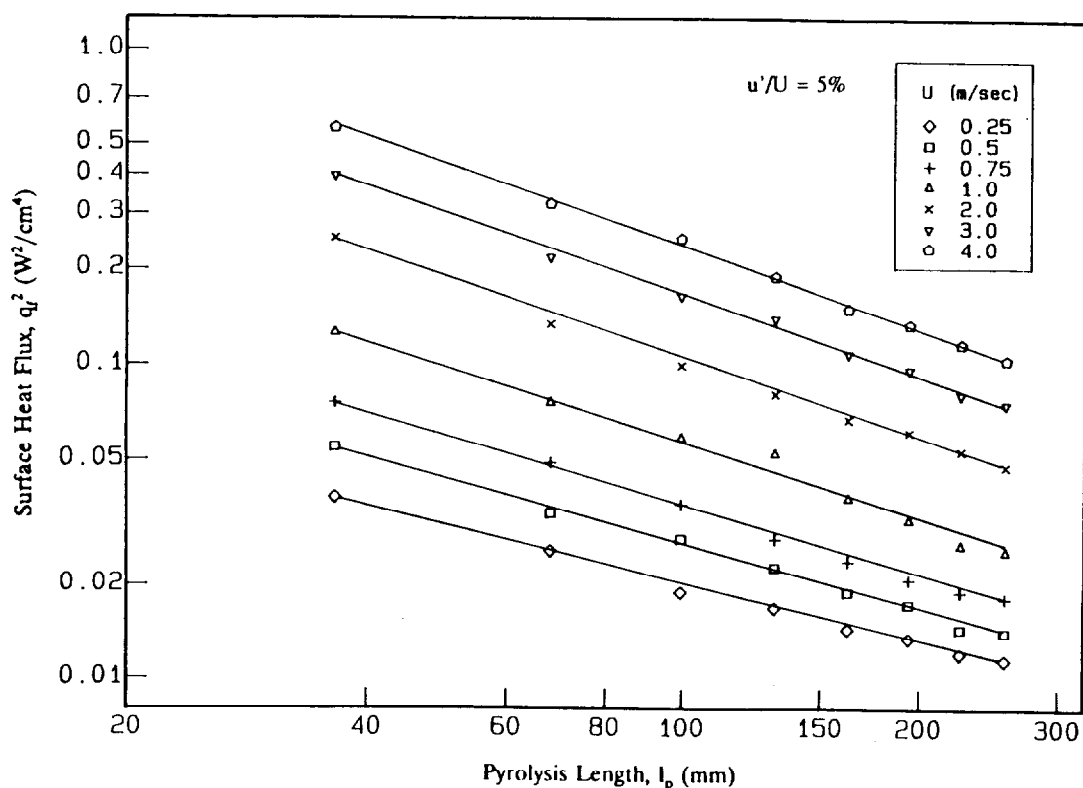


Fig. 5. Dependence of the surface heat flux on the pyrolysis length for several flow velocities and a turbulence intensity of 5% for ceiling flame spread.

velocity larger than 1 m/s, the flame propagates faster in the ceiling than in the floor, and that the difference is more pronounced for high turbulence intensities. This seems to be the result of the enhancement of the surface heat flux in the ceiling case due to the smaller flame standoff distance. For all the turbulence intensities tested, the enhancing effect of buoyancy on the flame spread becomes less significant as the flow velocity is increased. Because of the extinction of the flame at high

flow velocities, data could not be obtained for velocities larger than 5 m/s. However, ceiling and floor rates should become identical if the flow velocities were large enough to overcome buoyancy. For flows slower than 1 m/s, however, the opposite trend is observed. The flame propagates at a slower rate over the ceiling, which suggests that mechanisms other than the enhanced heat transfer effect discussed above are important at low velocity flows. During the experiments, it was visually observed that in

TABLE 2
The Dependence of c and d in Eq. 3, $q_f^2 l_p^c = d$, on the Flow Conditions (Ceiling)

Turbulence Intensity		Flow Velocity U (m/s)						
		0.25	0.5	0.75	1.0	2.0	3.0	4.0
1%	c	0.68	0.68	0.74	0.79	0.74	0.78	0.83
	d	0.4	0.5	0.7	1.2	3.6	6.0	8.5
5%	c	0.70	0.72	0.78	0.84	0.84	0.84	0.84
	d	0.6	0.65	1.3	2.0	6.0	9.0	9.8
10%	c	0.80	0.81	0.84	0.85	0.85	0.85	0.86
	d	0.75	1.5	2.0	3.5	8.2	9.5	10.0
15%	c	0.78	0.74	0.80	0.82	0.85	0.85	0.87
	d	1.0	2.1	2.4	5.4	8.5	9.8	10.2

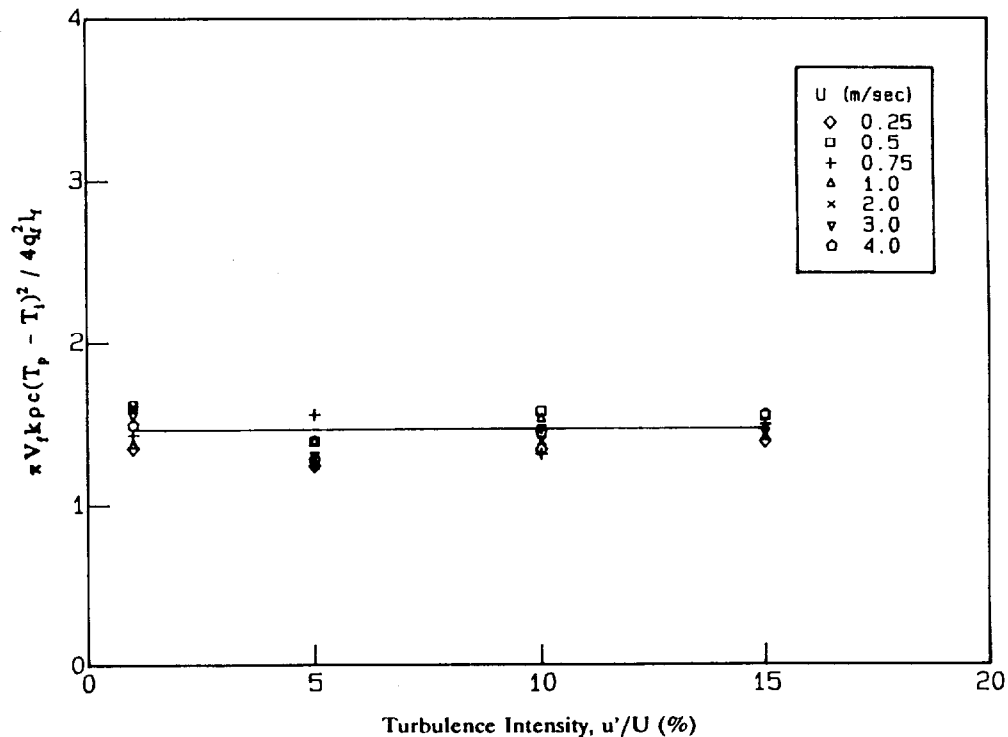
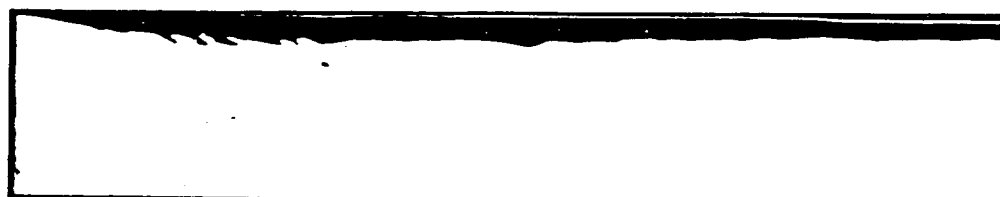


Fig. 6. Correlation of the ceiling flame spread data in terms of a nondimensional flame spread rate deduced from eq. 1.

$U = 2 \text{ m/sec}$, $u'/U = 1\%$



a) Ceiling



b) Floor

Fig. 7. Schlieren images of the flame spread process in (a) ceiling and (b) floor case under the flow condition of $U = 2 \text{ m/s}$ and $u'/U = 1\%$.

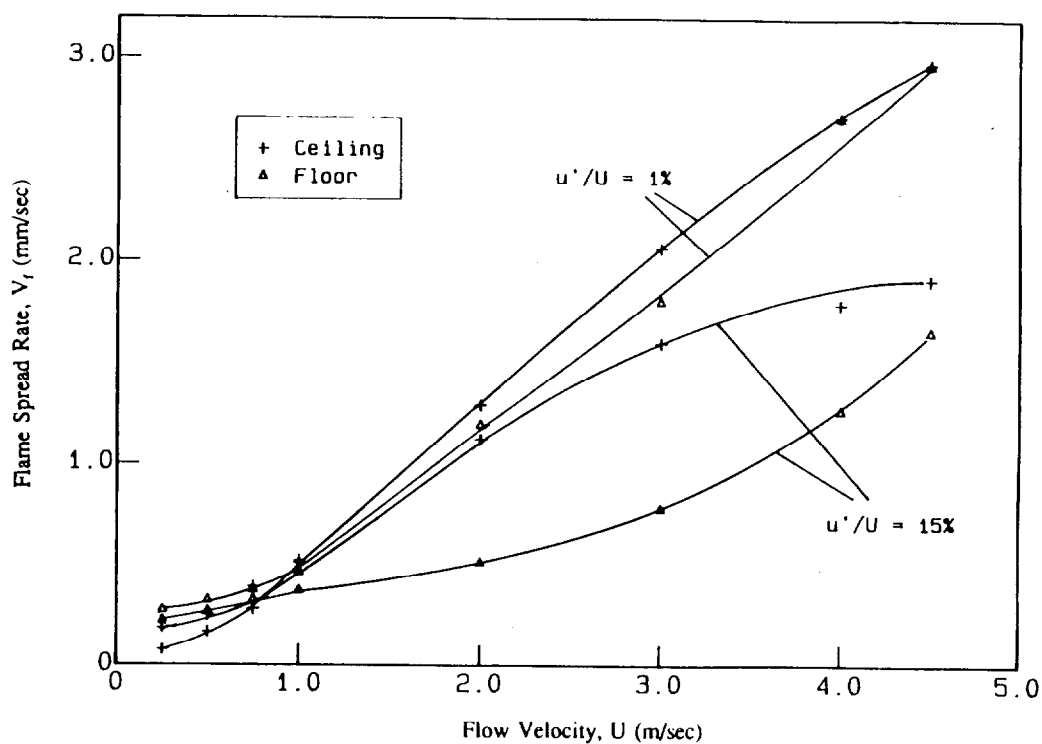


Fig. 8. Comparison of PMMA flame spread rate in floor and ceiling configurations.

the low flow velocity range, flames spreading across the ceiling were thin and weak and displayed a distinct blue color, unlike in the floor tests where thick and yellow flames were always observed. These visual observations agree with those of Mekki et al. [11]. Since the blue color in a flame is mainly emitted by CO at low temperature and the yellow is caused by soot at higher temperature, this observation suggests that the ceiling flames may be near extinction, probably due to heat loss to the wall and stratification effects.

To investigate the completeness of combustion in each case, the concentration of the major species O_2 , CO, CO_2 , NO, and gaseous unburned hydrocarbons (HC) in the exhaust flow were measured under various flow conditions. Some results are shown in Figs. 9–12 for flows with velocity of 1 m/s and turbulence intensity of 1% (Figs. 9 and 10) and 15% (Figs. 11 and 12). The experimental data are presented as functions of the pyrolysis front position to simplify the comparison between the different cases. The NO result is not presented

here due to its small value (less than 3 ppm) compared with other species. The CO and unburned hydrocarbons produced in volume per unit mass of fuel pyrolyzed are plotted in Figs. 9 and 11 while the consumed oxygen and produced CO_2 in volume per unit mass of PMMA pyrolyzed are compared between the floor and ceiling tests in Figs. 10 and 12. From Figs. 9 and 11, it is seen that much more CO and unburned hydrocarbons are measured for the ceiling cases. Less oxygen is consumed and less carbon dioxide is produced in the ceiling than in the floor, as shown in Figs. 10 and 12. Similar trends were observed for other tests with different velocities and turbulence intensities. A good indication of the completeness of the combustion is the CO concentration. From these measurements, it can be concluded at least for the flow conditions tested, that the chemical reactions are less complete in the ceiling flame spread. The measurements of O_2 , CO_2 and unburned hydrocarbons support this conclusion. In the floor case the unburned hydrocarbons are almost undetectable in most

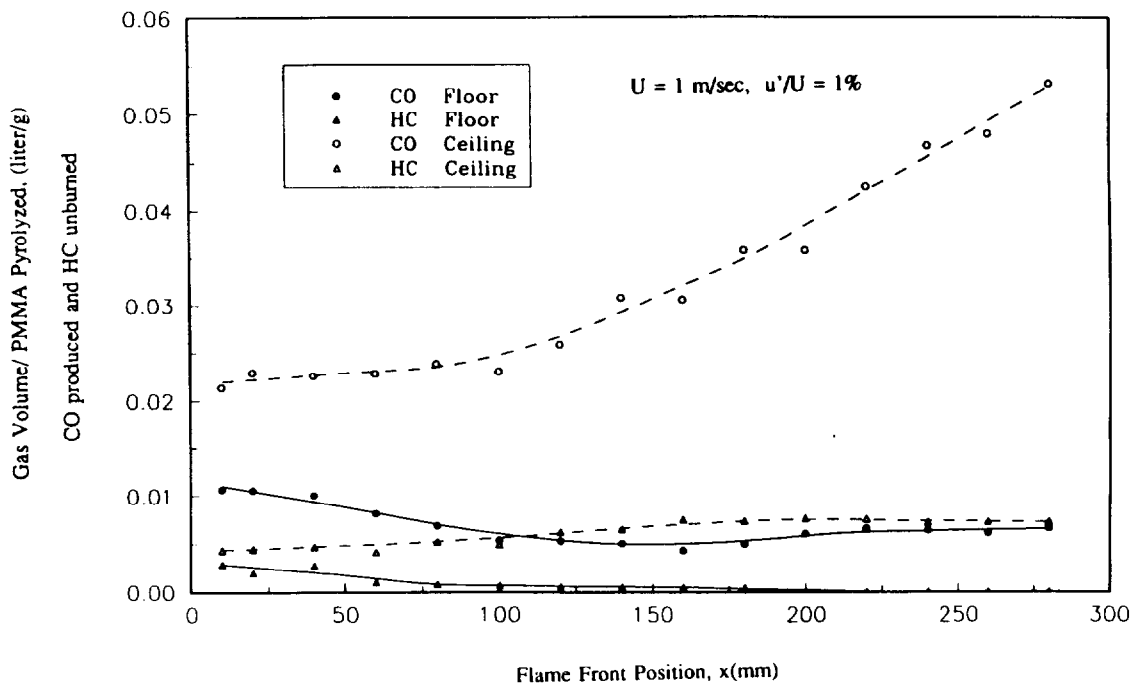


Fig. 9. Comparison of the exhaust gas composition measurements in ceiling and floor flame spread in air flow with velocity of 1 m/s and turbulence intensity of 1%. The data are presented as the produced CO and unburned HC (gas volume) per unit mass of the PMMA pyrolyzed.

conditions, including the low flow velocity cases. On the other hand, for ceiling flame spread, unburned hydrocarbons are found in all flow conditions, even for velocities as high as 4 m/s.

The observed differences in the combustion completeness in the floor and ceiling cases seem to be the result of the buoyancy effect on the respective flames and thermal layers. In ceiling spread the hot gases are above the cold air, and consequently, the thermal layer is thin and very stable. This deters the turbulent mixing of the fuel vapor and oxidizer at the mixing layer. In the floor case, the opposite effect takes place. The thermal layer is thick and unstable due to buoyancy-generated instabilities, which facilitate the mixing of fuel and oxidizer, and hence more complete chemical reactions. Another important cause for a weaker reaction in the ceiling flame spread is the quenching effect that the relatively low temperature surface has on the flame, which is more important in this case because the flame is closer to the fuel surface. The overall result

is that the ceiling combustion takes place under locally underventilated conditions, resulting in the observed presence of larger concentrations of CO and unburned hydrocarbons in the exhaust gases.

These phenomenological descriptions can be used to explain the observed flame spread rate variations in the ceiling and floor cases at low flow velocities. The effect of buoyancy on combustion appears to be the dominant mechanism and determines the magnitude of the flame spread rate at flows with low velocities. Since combustion is less complete in the ceiling case and consequently less heat is generated, the flame spreads slower in this configuration. At relatively high flow velocities, there is a larger supply of oxidizer to the reacting zone; thus the combustion reaction is more vigorous and the buoyancy effect appears to come primarily through the variation in the flame standoff distance. In the ceiling spread the flame is closer to the wall; therefore the surface heat flux is larger and consequently the spread rate is also larger.

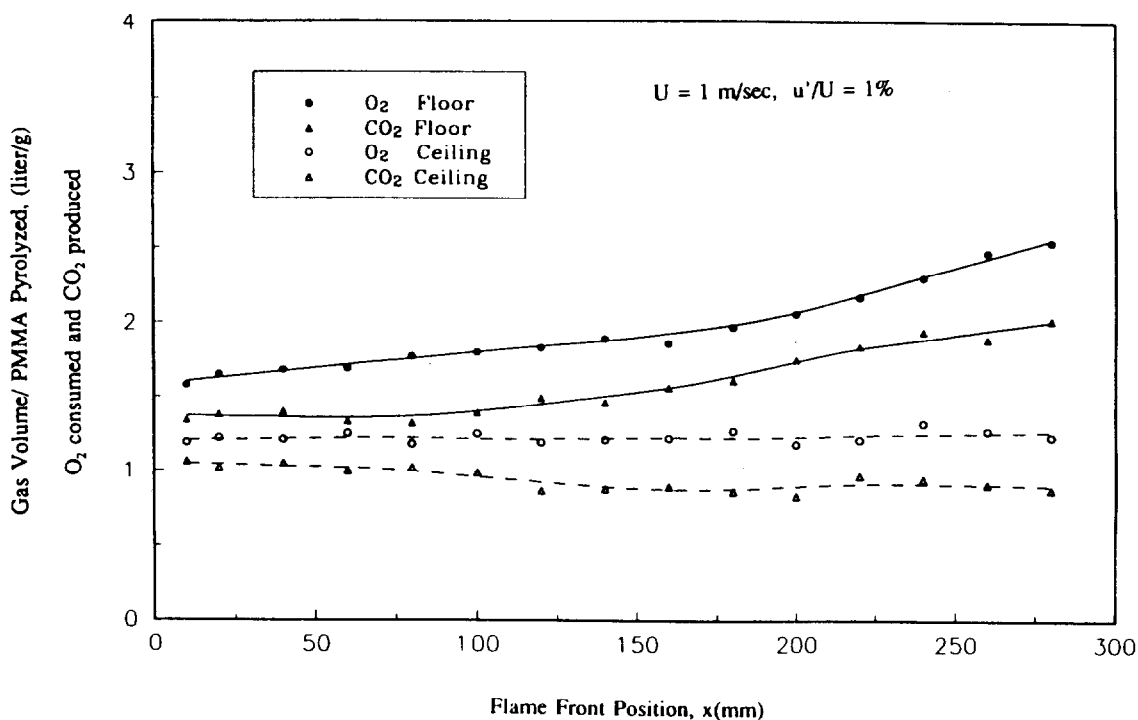


Fig. 10. Comparison of the exhaust gas composition measurements in ceiling and floor flame spread in air flow with velocity of 1 m/s and turbulence intensity of 1%. The data are presented as the produced CO_2 and consumed O_2 (gas volume) per unit mass of the PMMA pyrolyzed.

The turbulence effect discussed in the last section can also be studied with the gas concentration measurements in the exhaust flows. Comparison of the gas composition data for low-turbulence flow (Figs. 9 and 10) with those in the high-turbulence flows (Figs. 11 and 12) reveals that the flow turbulence reduces the CO and HC concentrations, and increases the oxygen consumption and CO_2 production in both floor and ceiling cases. These observations indicate that the primary effect of flow turbulence on horizontal flame spread is to enhance the combustion through stronger mixing of fuel vapor and oxidizer. The enhancing effect of turbulence on the combustion reactions results in a shortened flame, which, in turn, causes a smaller flame spread rate, as indicated by Eq. 1 and the experimental results.

CONCLUSION

The experiments conducted in this work on flame spread over a solid fuel surface in a

ceiling configuration show that the general features of the ceiling flame spread process are similar to those of floor spread. However, buoyancy creates some significant dissimilarities between the two processes. The most interesting differences caused by buoyancy are on the flame standoff distance and the stratification of the thermal layer. Buoyancy pushes the flame closer to the solid surface in the ceiling case and lifts the flame away from the surface in the floor case. A closer flame enhances the heat transfer to the surface from the flame, but results in less-complete combustion due to flame quenching by the wall and the poor mixing of the fuel and oxidizer, and consequently in a smaller heat release. The above mechanisms have opposite effects on the flame spread rate and the overall result depends on which effect is dominant. The experimental data suggest that in ceiling spread at low flow velocities, the flame quenching is the dominant mechanism and at large flow velocities the enhancing of the heat transfer becomes dominant. The differences between ceil-

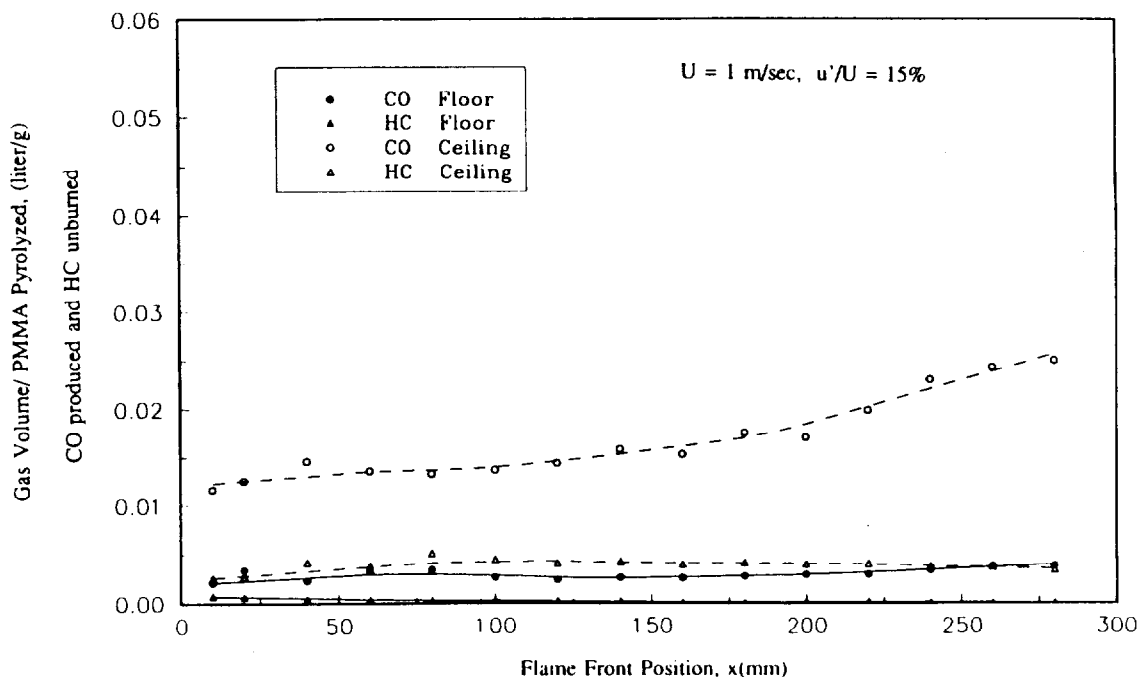


Fig. 11. Comparison of the exhaust gas composition measurements in ceiling and floor flame spread in air flow with velocity of 1 m/s and turbulence intensity of 15%. The data are presented as the produced CO and unburned HC (gas volume) per unit mass of the PMMA pyrolyzed.

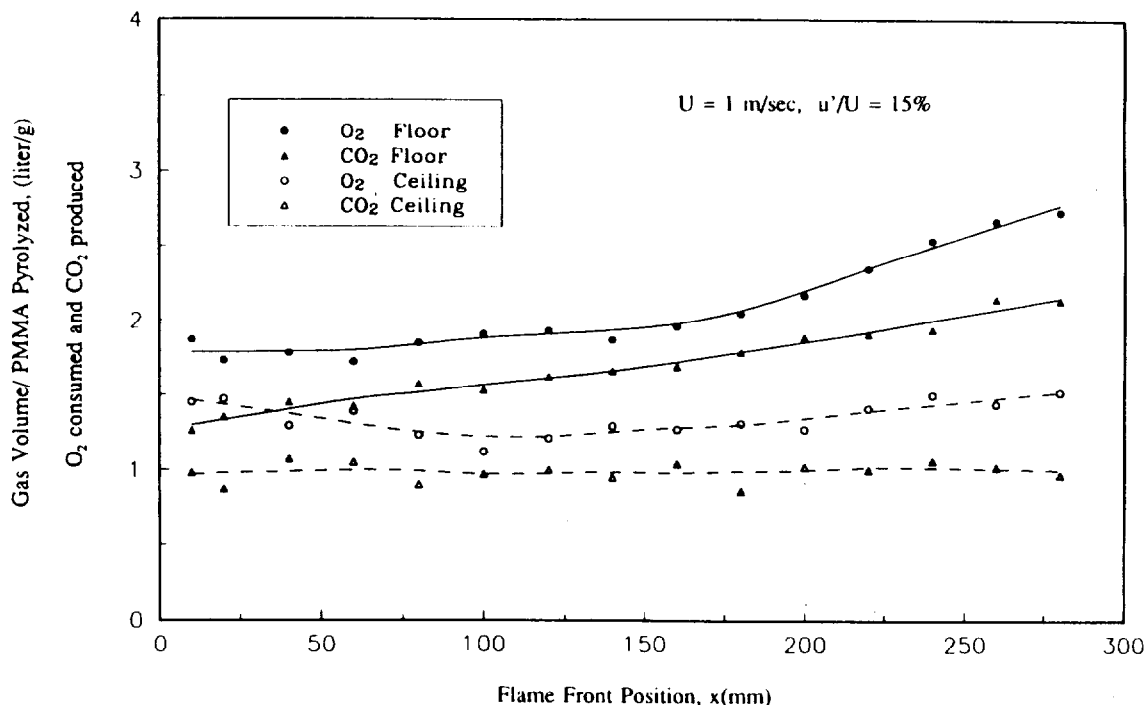


Fig. 12. Comparison of the exhaust gas composition measurements in ceiling and floor flame spread in air flow with velocity of 1 m/s and turbulence intensity of 15 %. The data are presented as the produced CO_2 and consumed O_2 (gas volume) per unit mass of the PMMA pyrolyzed.

ing and floor flame spread diminish as the flow velocity is increased. These experimental results indicate that care should be taken when using data obtained from either the floor or ceiling configuration to model or predict actual fire spread, or to design tests for material flammability ranking.

The observed incomplete combustion in ceiling flame spread is of particular importance in the theoretical modeling of flame spread since most current models assume complete combustion. It should be also important in the prediction of smoke formation and the toxicity of the combustion products in building fires.

This work was supported by the National Institute of Standards and Technology under Grant No. 60NANB7D0737. Partial funds for the experimental facility were provided by a National Science Foundation Research Grant. CBT-8506292.

REFERENCES

1. Sirignano, W. A., *Combust. Sci. Technol.* 6:95-105 (1972).
2. Williams, F. A., *Sixteenth Symposium (International) on Combustion*, The Combustion Institute, 1976, pp. 1281-1294.
3. Fernandez-Pello, A. C., and Hirano, T., *Combust. Sci. Technol.* 32:1-31 (1983).
4. Drysdale, D., *An Introduction to Fire Dynamics*, Wiley, New York, 1985.
5. Annamalai, K., and Sibulkin, M., *Combust. Sci. Technol.* 19:185-193 (1979).
6. Saito, K., Quintiere, J. G., and Williams, F. A., *Proceedings of the First International Symposium on Fire Safety Science*, Hemisphere, New York, 1986, pp. 75-86.
7. Orloff, L., de Ris, J., and Markstein, G. H., *Fifteenth Symposium (International) on Combustion*, The Combustion Institute, 1974, pp. 183-192.
8. Loh, H. T., and Fernandez-Pello, A. C., *Twentieth Symposium (International) on Combustion*, The Combustion Institute, 1984, pp. 1575-1582.
9. Apte, V. B., Bilger, R. W., Green, A. G., and Quintiere, J. G., *Combust. Flame* 85:169-184 (1991).
10. Mao, C. P., and Fernandez-Pello, A. C., *Proceedings of the Eastern States Section of Combustion Institute*, Philadelphia, 1985, pp. 243-247.
11. Mekki, K., Atreya, A., Agrawal, S., and Wichman, I., *Twenty-Third Symposium (International) on Combustion*, The Combustion Institute, 1990, pp. 1701-1707.
12. Standard Method of Test for Surface Burning Char-

- acteristics of Building Materials, E84-70, Book of ASTM Standards, Philadelphia, Part 14, p. 472, 1973.
13. Zhou, L., and Fernandez-Pello, A. C., *Twenty-Third Symposium (International) on Combustion*, The Combustion Institute, Pittsburgh, 1990, pp. 1709-1714.
 14. Zhou, L., Fernandez-Pello, A. C., and Cheng, R., *Combust. Flame* 81:40-49 (1990).
 15. Zhou, L., and Fernandez-Pello, A. C., *Twenty-Fourth Symposium (International) on Combustion*, The Combustion Institute, Pittsburgh, 1992, in press.
 16. Zhou, L., Ph.D thesis, University of California at Berkeley, 1991.
 17. Quintiere, J. G., *J. Fire Mater.* 5:52-60 (1981).
 18. Delichatsios, M. A., *Combust. Sci. Technol.* 39: 195-214 (1984).
 19. Hasemi, Y., *Proceedings of the First International Symposium on Fire Safety Science*, Hemisphere New York, 1986, pp. 87-96.
 20. Tu, K.-M., and Quintiere, J. G., 1988 Technical Meeting of Eastern Section of The Combustion Institute, Clearwater Beach, FL, December, 1988.
 21. Orloff, L., and de Ris J., *Combust. Flame* 18:389-401 (1972).

Received 29 January 1992, revised 7 August 1992